

DTFNPS (mean 1.771 Å), but slightly shorter than in a selection of unfluorinated diphenyl sulfides where the mean length is 1.780 Å. Such a shortening of bond lengths in fluorinated compounds has been noted previously (Goodhand & Hamor, 1979, and references therein).

With respect to the bond angle at S, Goodhand & Hamor (1979) noted that in the fluorinated compound DTFNPS this was 99.7°, significantly smaller than in unfluorinated analogues, where this angle ranged from 102.9 to 105.6, mean 103.7°. More recent studies have, however, revealed somewhat smaller C—S—C angles in a small number of diphenyl sulfide systems, the smallest value (101.2°) occurring in the crystal structure of 2-nitro-1,3-bis-(phenylthio)benzene (Lynch, Simonsen, Miller, Turley & Martin, 1985). The C—S—C angles in the title compounds, 102.0° in (I) and 99.7° in (II) are, nevertheless, still consistent with the overall trend noted previously.

There are no abnormal intermolecular contact distances in either structure. The shortest contact, 2.744 Å, occurs in structure (I), between F2' and F7'E of the disordered trifluoromethyl group of the molecule at $-x, \frac{1}{2} + y, -\frac{1}{2} - z$.

We thank Dr P. L. Coe and Professor J. C. Tatlow for suggesting this problem and for samples of the title compounds, the University of Birmingham for the award of a Research Studentship (to NG), and the staff of the University Computer Centre for their assistance.

References

- COE, P. L., MILNER, M. E., TATLOW, J. C. & WRAGG, R. T. (1972). *Tetrahedron*, **28**, 105–109.
 GOODHAND, N. & HAMOR, T. A. (1979). *J. Fluorine Chem.* **14**, 223–233.
 GOODHAND, N. & HAMOR, T. A. (1982). *Acta Cryst.* **B38**, 1342–1345.
International Tables for X-ray Crystallography (1974). Vol. IV. Birmingham: Kynoch Press. (Present distributor Kluwer Academic Publishers, Dordrecht.)
 KRAJEWSKI, A., RIVA DI SANSEVERINO, L., DONDONI, A. & MANGINI, A. (1975). *J. Cryst. Mol. Struct.* **5**, 345–351.
 LYNCH, V. M., SIMONSEN, S. H., MILLER, R. F., TURLEY, J. C. & MARTIN, G. E. (1985). *Acta Cryst.* **C41**, 1240–1242.
 MOTHERWELL, W. D. S. & CLEGG, W. (1978). *PLUTO*. Program for plotting molecular and crystal structures. Univ. of Cambridge, England.
 SHELDRIK, G. M. (1976). *SHELX76*. Program for crystal structure determination. Univ. of Cambridge, England.
 VAN DER HEIJDEN, S. P. N., GRIFFITH, E. A. H., CHANDLER, W. D. & ROBERTSON, B. E. (1975). *Can. J. Chem.* **53**, 2084–2092.

Acta Cryst. (1989). **C45**, 1612–1616

Malotilate: Structure and Phase Transformation

BY D. R. VEGA AND R. F. BAGGIO*

Departamento de Física, Comisión Nacional de Energía Atómica, Av. del Libertador 8250, Buenos Aires 1429, Argentina

(Received 13 July 1988; accepted 27 February 1989)

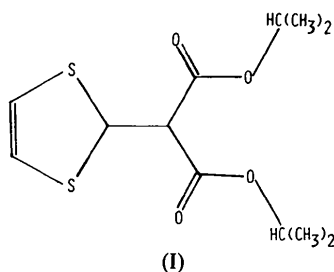
Abstract. C₁₂H₁₆O₄S₂, *M*_r = 288.4. Two phases: phase *A*: monoclinic, *P*2₁/*a*, *a* = 22.425 (3), *b* = 8.273 (2), *c* = 15.713 (3) Å, β = 96.66 (1)°, *V* = 2895 (1) Å³, *Z* = 8, *D*_x = 1.323, *D*_m = 1.320 (2) g cm⁻³, Mo *K*α radiation, λ = 0.7107 Å, μ = 3.55 cm⁻¹, *F*(000) = 1216, final conventional *R* factor = 0.071, for 1404 observed [*I* > 2σ(*I*)] reflexions out of 4530 unique; phase *B*: triclinic, *P*1̄, *a* = 11.515 (2), *b* = 11.840 (2), *c* = 12.097 (2) Å, α = 94.57 (2), β = 102.91 (2), γ = 100.81 (2)°, *V* = 1566 (1) Å³, *Z* = 4, *D*_x = 1.212, *D*_m = 1.215 (2) g cm⁻³, Mo *K*α radiation, λ = 0.7107 Å, μ = 3.28 cm⁻¹, *F*(000) = 608, final conventional *R* = 0.059, for 2338 observed [*I* > 3σ(*I*)] reflexions out of 4585 unique. Data gathered at room temperature. In

both structures the asymmetric unit consists of two independent moieties, which in form *A* are found to pack more closely than in form *B*, as seen from the measured density values. This is achieved through an overall greater departure of the molecule from planarity giving rise to a geometry more amenable to dense stacking. Intermolecular interactions are mainly van der Waals, with only a few weak hydrogen bonds present (shortest O...H: 2.32 Å).

Introduction. Malotilate [C₁₂H₁₆O₄S₂, diisopropyl 1,3-dithiol-2-ylidenemalonate, (I)] is a very powerful hepatoprotector and activator, which in the last few years has merited the increasing attention of a number of research workers in the field of biology, to the point of having specific meetings organized on the subject (Symposium on Malotilate held at the 7th

* Author to whom correspondence should be addressed.

World Congress of Gastroenterology, Stockholm, 1982). But in spite of the large amount of entries on related topics available in the literature, very little has been reported regarding the study of the molecule from a physico-chemical point of view. The only data we could trace was a Patent (Nihon Nohyaku Co. Ltd, 1984), where two crystallographic phases, *A* and *B*, are mentioned, each characterized by its melting point (*A*: 325 K; *B*: 335 K) and three prominent peaks from each X-ray powder diffraction data.



In order to achieve a synthetic route oriented to the obtention of the pharmacologically more suitable phase *A*, a thorough understanding of the physico-chemical behaviour of the molecule is required, so as to be able to achieve this on rational, rather than empirical, terms. It was as a first step along this line of thought that the present work on malotilate was undertaken.

Experimental. Material. The raw material used throughout this investigation was supplied by Laboratories Laplex Argentina, and this is gratefully acknowledged. A 5 g sample of pharmacological purity, identified as belonging to form *A*, was supplied.

The compound was found to be almost indefinitely soluble in any organic solvent we tried (acetone, ethanol, toluene, benzene, *etc.*). Trials to recrystallize it usually proved unsuccessful due to the solutions going into a syrup like state, without any nucleation. Seeding did not work, as the seed would dissolve almost instantaneously, whatever the state of concentration. Occasionally, the syrup would suddenly crystallize overnight, into a solid bowl in which very large interwoven single crystals coexisted embedded in a solid, polycrystalline matrix. The material thus obtained was always identified as phase *A*, irrespective of the solvent used or the crystallization temperature.

A single exception was found to this, when a trial with a saturated solution from a 50% mixture of ethanol-water produced very thin phase *B* plates, on cooling. Later attempts to reproduce this result were unsuccessful.

The only reproducible way we found of obtaining single-crystal material was by cooling from the melt

after seeding the suitable crystal type at the correct temperature (crystals of phase *B* in the range $325 < T < 335$ K, or those of phase *A* at $T < 325$ K). With this technique, and by accurate control of the growth temperature, large single crystals could be obtained almost at will. Specimens of both forms were easily recognized at the polarizing microscope by the striking pleochroism displayed by crystals of phase *B*, in contrast to the very low pleochroism shown by those of phase *A*.

Phase transformation. While trying to reproduce the reported melting temperatures of both phases, it was observed that most specimens melted at $T = 335$ K (the reported value for phase *B*), and very few at $T = 325$ K (that for phase *A*), even when the batch from which they were taken had been unambiguously identified as belonging to the latter. This suggested the existence of a temperature-induced *A*→*B* phase transition. To verify this a number of specimens of form *A* were inspected under crossed polars, while simultaneously heated on the heating stage of a polarizing microscope: at temperatures ranging from 303 to 323 K, a first-order transformation front could be seen running across many of the crystals observed, leaving behind it a coloured, polycrystalline specimen, clearly identifiable as belonging to form *B*. On further heating, these crystals melted at 335 K. Those which did not transform, instead, melted much earlier, at 325 K. At temperatures between the two melting points, solid material of phase *B* in contact with the liquid acted as a seed triggering a fast nucleation and growth process. This suggested the method of growing single crystals from the melt, especially when the observation was made that the liquid phase could stay almost indefinitely in a metastable state even at room temperature, with the sole requirement of being left unperturbed.

The reverse transformation *B*→*A* was never observed, even down to liquid N₂ temperatures.

Thermal analysis (DSC) of the transformation did not provide much clarification. On heating, the diagrams obtained showed very broad peaks, with many irreproducible, sample dependent features which obscured the analysis.

At this stage it seemed that some structural work should be performed in order to gain some understanding of the problem, and so the crystal structure analysis of both phases was undertaken.

Structure resolution. Suitable specimens for single-crystal X-ray diffraction could be obtained by cutting them from a solidified droplet, slowly grown from the melt. Utmost care was exercised in avoiding excessive pressing and deformation. The final choice was made on the grounds of the best optical extinction. In this way, samples of both *A* and *B* phases were readily available for crystallographic purposes,

Table 1. Fractional atomic positions and equivalent isotropic temperature factors

$$B_{eq} = \frac{1}{3} \pi^2 \sum_i \sum_j (a_i^* a_j^*) (\mathbf{a}_i \cdot \mathbf{a}_j) U_{ij}$$

	Phase A				Phase B			
	x	y	z	$B_{eq}(\text{\AA}^2)$	x	y	z	$B_{eq}(\text{\AA}^2)$
S11	0.4186 (4)	0.0801 (12)	0.4038 (5)	2.50	0.1577 (1)	0.4526 (1)	0.1609 (2)	4.09
S12	0.5347 (4)	0.2055 (12)	0.3760 (6)	2.77	-0.0885 (1)	0.4687 (1)	0.1650 (2)	3.94
O11	0.4430 (10)	0.3348 (29)	0.6478 (17)	2.64	0.0534 (4)	0.0879 (5)	0.1957 (5)	7.67
O12	0.5556 (10)	0.3582 (28)	0.6398 (15)	2.84	-0.1554 (6)	0.1087 (5)	0.2184 (6)	7.58
O13	0.3921 (9)	0.1661 (25)	0.5539 (14)	2.74	0.1867 (5)	0.2417 (4)	0.1852 (5)	7.84
O14	0.5790 (9)	0.3754 (28)	0.5055 (14)	3.02	-0.2068 (4)	0.2733 (4)	0.2009 (5)	8.53
C11	0.4433 (16)	0.0324 (41)	0.3054 (20)	3.46	0.1199 (6)	0.5855 (5)	0.1446 (6)	4.30
C12	0.4976 (16)	0.0931 (41)	0.2971 (20)	3.40	0.0052 (6)	0.5928 (5)	0.1475 (5)	4.43
C13	0.4807 (12)	0.1930 (36)	0.4484 (25)	2.68	0.0156 (5)	0.3805 (5)	0.1703 (5)	3.03
C14	0.4869 (20)	0.2601 (43)	0.5292 (21)	2.61	-0.0108 (5)	0.2652 (6)	0.1834 (5)	3.42
C15	0.4358 (17)	0.2453 (53)	0.5776 (29)	2.73	0.0834 (7)	0.1961 (7)	0.1878 (6)	4.72
C16	0.5425 (17)	0.3367 (42)	0.5557 (28)	2.80	-0.1313 (7)	0.2166 (7)	0.1997 (7)	5.30
C17	0.3944 (15)	0.3281 (38)	0.7045 (21)	3.96	0.1478 (10)	0.0225 (7)	0.2103 (12)	10.50
C18	0.3430 (13)	0.4289 (41)	0.6668 (20)	5.15	0.1230 (13)	-0.0574 (12)	0.1087 (11)	19.79
C19	0.4197 (13)	0.4018 (48)	0.7873 (19)	4.77	0.1307 (15)	-0.0587 (12)	0.2916 (12)	21.67
C1A	0.6120 (14)	0.4441 (41)	0.6713 (21)	2.72	-0.2691 (9)	0.0606 (9)	0.2447 (11)	9.12
C1B	0.6641 (12)	0.3312 (38)	0.6747 (21)	4.77	-0.2472 (10)	-0.0218 (10)	0.3249 (11)	12.04
C1C	0.6005 (13)	0.5152 (41)	0.7552 (19)	3.81	-0.3523 (10)	0.0078 (9)	0.1345 (12)	12.38
S21	0.2809 (4)	0.2153 (11)	0.3169 (6)	2.56	-0.4212 (1)	0.3368 (2)	-0.0245 (2)	3.43
S22	0.1742 (4)	0.4073 (12)	0.3251 (6)	2.76	-0.6735 (1)	0.3272 (2)	-0.0235 (2)	3.84
O21	0.2424 (9)	0.2624 (25)	0.0424 (17)	2.52	-0.5407 (4)	0.3036 (4)	-0.3942 (5)	4.15
O22	0.1302 (10)	0.3009 (28)	0.0560 (16)	2.93	-0.7375 (4)	0.3720 (4)	-0.3798 (4)	4.10
O23	0.2893 (9)	0.1390 (26)	0.1574 (13)	2.29	-0.3979 (4)	0.3363 (5)	-0.2359 (4)	3.94
O24	0.1140 (10)	0.4365 (30)	0.1726 (14)	2.96	-0.8051 (4)	0.3124 (4)	-0.2315 (4)	4.17
C21	0.2675 (16)	0.2854 (39)	0.4148 (21)	3.35	-0.4552 (6)	0.3379 (6)	0.1050 (6)	4.06
C22	0.2170 (14)	0.3718 (44)	0.4210 (22)	3.35	-0.5741 (6)	0.3354 (6)	0.1064 (6)	4.28
C23	0.2166 (12)	0.3013 (40)	0.2610 (24)	2.37	-0.5686 (5)	0.3323 (4)	-0.1058 (6)	3.35
C24	0.2030 (17)	0.2925 (44)	0.1714 (24)	2.19	-0.5982 (5)	0.3326 (5)	-0.2228 (6)	2.93
C25	0.2493 (16)	0.2199 (48)	0.1238 (26)	2.24	-0.5040 (7)	0.3262 (6)	-0.2835 (7)	3.62
C26	0.1452 (17)	0.3542 (45)	0.1334 (27)	2.54	-0.7196 (7)	0.3364 (6)	-0.2764 (7)	3.98
C27	0.2862 (13)	0.2043 (38)	-0.0107 (18)	2.64	-0.4510 (8)	0.3001 (10)	-0.4596 (7)	5.04
C28	0.3423 (13)	0.3028 (37)	0.0011 (17)	3.72	-0.4991 (9)	0.3290 (10)	-0.5738 (8)	7.39
C29	0.2563 (13)	0.2012 (39)	-0.1006 (17)	3.26	-0.4342 (11)	0.1838 (11)	-0.4694 (10)	14.67
C2A	0.0720 (13)	0.3455 (38)	0.0120 (19)	3.11	-0.8601 (7)	0.3808 (8)	-0.4410 (7)	5.13
C2B	0.0270 (13)	0.2204 (42)	0.0287 (22)	6.16	-0.9203 (10)	0.2653 (10)	-0.5020 (8)	8.63
C2C	0.0774 (12)	0.3785 (43)	-0.0800 (17)	3.27	-0.8454 (8)	0.4676 (9)	-0.5193 (8)	9.61

although the data collection evidenced a poor diffraction power for both samples.

A summary of relevant data follows. Preliminary information (symmetries and space groups): from precession and Weissenberg photographs. Systematic absences: $(h0l)$, $h = 2n$; $(0k0)$, $k = 2n$ for phase *A*, and none for phase *B*. Intensity data: from an Enraf-Nonius CAD-4 diffractometer, ω - 2θ scan mode, $2\theta_{\max} = 50^\circ$; three standard reflections, no significant intensity variation. Crystal size: $0.15 \times 0.06 \times 0.25$ mm (phase *A*), $0.22 \times 0.28 \times 0.35$ mm (phase *B*). Density measurements: by flotation in an aqueous solution of sodium thiosulfate (determination of the liquid density through the measurement of its refractive index). Cell parameters: by refinement of 25 (phase *A*) and 36 (phase *B*) reflexions in the range $13 < 2\theta < 22^\circ$ (Mo $K\alpha$ radiation, $\lambda = 0.7107$ Å). Data set (phase *A*): 4530 unique reflexions collected, only 31% of which [1404 with $I > 2\sigma(I)$] used in refinement; $-23 \leq h \leq 22$, $0 \leq k \leq 7$, $0 \leq l \leq 15$. Data set (phase *B*): 4585 unique reflexions collected, 51% of which [2338 with $I > 3\sigma(I)$] used in refinement; $-12 \leq h \leq 12$, $-11 \leq k \leq 12$, $0 \leq l \leq 13$. Model refinement: by full-matrix least squares (on F^2 's), using the *SHELX76* package (Sheldrick, 1976), and form factors therein; $R_A = 0.071$, $wR_A = 0.073$, $w_A = 3.32/[\sigma^2(F) + 0.000476 \times F^2]$, R_B

$= 0.059$, $wR_B = 0.061$, $w_B = 2.78/[\sigma^2(F) + 0.000564 \times F^2]$. $(\Delta/\sigma)_{\max}$ in final cycle: 0.015. Total number of parameters refined $N = 325$. No extinction or absorption corrections made. Poor diffraction power of the samples determined a rapid fall-off of the intensities with increasing Bragg angle.

Both structures were solved in a rather straightforward way, with the help of the *SHELX86* package (Sheldrick, 1986): form *A* by means of direct methods; form *B* using a Patterson search. The methods were shown to be equally efficient, in spite of the rather uneven quality of the data employed.

Model completion was carried out by means of ΔF synthesis. Difficulties in finding the methyl C atoms were interpreted as a sign of positional disorder, later confirmed by the full-matrix least-squares refinement. Isotropic refinement of all other non-H atoms converged smoothly to reasonable values, but again, the terminal CH_3 groups drifted erratically, with a dramatic rise in temperature factors.

In order to overcome this a constrained refinement was then attempted where the C— CH_3 bond length was restricted to have a uniform, though refinable, value with a fixed standard deviation $\sigma = 0.01$ Å. As a result there was a general improvement in the geometry (angles included) of the terminal groups. Thermal factors nonetheless remained abnormally

large, mainly in phase *B*. At this stage the discrepancy indices were $R_A(\text{iso.}) = 0.131$ and $R_B(\text{iso.}) = 0.091$. Inclusion of anisotropic temperature factors caused an important *R* factor drop: $R_A(\text{anis.}) = 0.071$, $R_B(\text{anis.}) = 0.059$. These final *R* indices refer to models including the H atoms at their expected positions. An *R* factor was calculated with the fully refined models but with the H atoms removed. This resulted in R_A increasing from 0.071 to 0.100, and R_B from 0.059 to 0.073. The contribution was considered significant, and the inclusion of the H atoms appropriate.

A final ΔF synthesis did not show any significant structure attributable to unaccounted for electron density, with departures from zero of less than $0.5 \text{ e } \text{Å}^{-3}$.

Discussion. Final atomic parameters and equivalent isotropic temperature factors are given in Table 1, while Table 2 shows interatomic distances and angles.*

The reported results clearly reflect the fact that the data set for form *A* was of an obvious poorer quality than that for form *B* [only 31% of the whole data set fulfilled the condition $I_A > 2\sigma(I_A)$, against 51% with $I_B > 3\sigma(I_B)$ used in the refinement of form *B*]. This was evidenced in the much higher e.s.d.'s from least squares. The molecular structure obtained, however, is essentially fair with high but still normal temperature factors. Form *B*, instead, with a better quality (and much larger) data set was more poorly defined, with abnormally large temperature factors strongly suggesting some kind of positional disorder, in agreement with the fact that crystals of form *B* can not be grown from the melt below 325 K, and so it should be considered as a metastable state at room temperature. The spatial disorder shown is therefore a manifestation of the kind of stresses involved.

In spite of these problems the constrained refinement led to reasonable molecular geometries for both forms, in good agreement with each other. The dithiole groups did not differ substantially from those reported in the literature (e.g. Bonnaud, Proutiere, Viani, Monnier, Bodot & Aycard, 1987; Geiser, Wang, Hammond, Firestone, Beno, Carlson, Nuñez & Williams, 1987; Kawamoto, Tanaka & Tanaka, 1987).

Although there are no relevant gross features differentiating the two types of molecules, there are

Table 2. Interatomic bonds (Å) and angles (°)

	Phase <i>A</i>		Phase <i>B</i>	
	Mol. 1	Mol. 2	Mol. 1	Mol. 2
S1—C1	1.75 (4)	1.70 (4)	1.72 (1)	1.70 (1)
S1—C3	1.75 (3)	1.75 (3)	1.73 (1)	1.75 (1)
S2—C2	1.69 (3)	1.72 (3)	1.71 (1)	1.71 (1)
S2—C3	1.76 (4)	1.71 (4)	1.73 (1)	1.73 (1)
O1—C5	1.32 (4)	1.32 (5)	1.28 (1)	1.30 (1)
O1—C7	1.49 (4)	1.44 (4)	1.44 (1)	1.44 (1)
O2—C6	1.33 (5)	1.30 (5)	1.31 (1)	1.34 (1)
O2—C4	1.48 (4)	1.45 (4)	1.44 (1)	1.47 (1)
O3—C5	1.20 (4)	1.19 (4)	1.22 (1)	1.21 (1)
O4—C6	1.24 (5)	1.20 (5)	1.20 (1)	1.23 (1)
C1—C2	1.34 (5)	1.35 (5)	1.35 (1)	1.37 (1)
C3—C4	1.38 (5)	1.41 (5)	1.37 (1)	1.38 (1)
C4—C5	1.45 (6)	1.48 (6)	1.47 (1)	1.45 (1)
C4—C6	1.42 (5)	1.46 (5)	1.46 (1)	1.41 (1)
C7—C8	1.49 (4)	1.49 (4)	1.43 (2)	1.46 (1)
C7—C9	1.49 (4)	1.49 (4)	1.45 (2)	1.43 (2)
C _A —C _B	1.49 (4)	1.49 (5)	1.45 (2)	1.47 (1)
C _A —C _C	1.49 (5)	1.49 (4)	1.47 (2)	1.46 (1)
C3—S1—C1	98 (2)	95 (2)	96.4 (3)	97.0 (3)
C3—S2—C2	97 (2)	98 (2)	97.0 (3)	97.4 (3)
C7—O1—C5	117 (3)	118 (3)	117.8 (6)	118.6 (6)
C _A —O2—C6	118 (3)	119 (3)	120.3 (7)	120.1 (6)
C1—C2—S2	120 (3)	115 (3)	116.6 (5)	116.2 (6)
C2—C1—S1	113 (3)	119 (3)	116.6 (5)	116.8 (5)
S2—C3—S1	110 (2)	113 (2)	113.3 (4)	112.4 (4)
C4—C3—S1	125 (3)	124 (3)	123.3 (5)	124.0 (5)
C4—C3—S2	125 (3)	123 (3)	123.3 (5)	123.5 (4)
C3—C4—C6	116 (3)	118 (3)	118.0 (7)	117.8 (7)
C3—C4—C5	117 (3)	116 (3)	120.0 (6)	118.1 (6)
C5—C4—C6	127 (3)	126 (3)	121.9 (7)	124.0 (7)
O1—C5—O3	125 (4)	125 (4)	121.8 (8)	120.7 (8)
O1—C5—C4	111 (4)	112 (3)	117.8 (7)	116.0 (6)
O3—C5—C4	123 (3)	123 (4)	120.5 (7)	123.2 (7)
O2—C6—O4	121 (3)	125 (3)	118.9 (7)	120.3 (6)
O2—C6—C4	116 (4)	113 (3)	118.7 (7)	116.2 (7)
O4—C6—C4	123 (4)	122 (4)	122.4 (7)	123.4 (7)
O1—C7—C8	109 (3)	112 (2)	107 (1)	108.7 (8)
O1—C7—C9	106 (3)	107 (2)	110 (1)	106.8 (9)
C8—C7—C9	109 (3)	114 (3)	99 (1)	108.9 (9)
O2—C _A —C _B	110 (3)	109 (3)	108 (1)	106.5 (8)
O2—C _A —C _C	105 (3)	110 (3)	105 (1)	107.2 (6)
C _B —C _A —C _C	115 (3)	116 (3)	113 (1)	112.1 (8)

some minor details which may be worth mentioning. The most conspicuous is perhaps the difference in the dihedral angle between the planes defined by O₃—C₅—C₄ and O₄—C₆—C₄, which in form *A* appears distinctly larger [24 (4)° average] than in form *B* [12 (9)°]. These different departures from coplanarity could be associated with different abilities to have a closer packing in the solid state: form *A* packs much more efficiently than does form *B* [$d_A = 1.32 \text{ g cm}^{-3}$, $V/Z = 361.9 (1) \text{ Å}^3 \text{ mol}^{-1}$; $d_B = 1.21 \text{ g cm}^{-3}$, $V/Z = 391.6 (1) \text{ Å}^3 \text{ mol}^{-1}$]. This is achieved through a dense stacking of molecules having their longer axis laying nearly parallel to each other (Fig. 1*a*). In form *B*, instead, the more planar molecules are found almost at right angles to each other (Fig. 1*b*) determining a much more open structure.

Surprisingly, the shortest C—H...O contact is found precisely in form *B* [C21—H21...O14 = 3.097 (9), H21...O14 = 2.32 Å, C21—H21...O14 = 127°], which according to the literature (Taylor & Kennard, 1982) should be considered a weak hydrogen bond.

There are five other weak H...O contacts: C11—H11...O23(−*x*, 1−*y*, −*z*) = 3.077 (8), H11...

* Tables of anisotropic thermal parameters, calculated positions of H atoms, observed and calculated structure factors, and the indexed powder diagrams for both phases have been deposited with the British Library Document Supply Centre as Supplementary Publication No. SUP 51992 (23 pp.). Copies may be obtained through The Executive Secretary, International Union of Crystallography, 5 Abbey Square, Chester CH1 2HU, England.

O23 = 2.48 Å, C11—H11...O23 = 114°; C12—H12...O24(-1-x, 1-y, -z) = 3.072 (9), H12...O24 = 2.47 Å, C12—H12...O24 = 114° and C22—H22...O13(x-1, y, z) = 3.15 (1), H22...O13 = 2.47 Å, C22—H22...O13 = 120°, all in form *B*, and C21—H21...O13 = 3.48 (4), H21...O13 = 2.46 Å, C21—H21...O13 = 157° and C12—H12...O24(0.5+x, 0.5-y, z) = 3.45 (4), H12...O24 = 2.50 Å, C12—H12...O24 = 146°, in form *A*. All the contacts found are long enough to be ascribed only slight hydrogen-bond character; the main source for crystal cohesion remains the usual van der Waals forces.

This encouraged an early idea of performing some comparative calculations on crystal lattice energies, as the potentials describing atom-atom interactions are only valid in the absence of strong hydrogen bonds. A minimization of the crystal lattice energy with respect to lattice constants, molecular translations, rotations and also subrotations of molecular fragments about selected bonds as axes was performed by means of the program *PCK3* (Williams, 1972, 1974) starting from the experimentally determined structure. Potential-energy functions of the form $U(r) = -Ar^{-6} + B\exp(-Cr)$ were used to

represent the non-bonded interatomic potential energy. The set of potential parameters included parameters fitted by Williams (1967) for C-H interactions, Bougeard (1984) for O-H, O-O and O-C, and Burgos & Righini (1983) for S-S and S-C. For mixed interactions, combination rules of Mirskaya (1973) were used.

Two runs of energy minimization were carried out for phases *A* and *B* with $\exp(-6-1)$ potential functions: in the first, the X-ray molecular structure was retained and the cell parameters were included as variables; in the second, subrotations about selected bonds taken as axes were relaxed (these subrotations were all performed on methyl groups). Both runs gave essentially the same results: apart from some minor changes in phase *B*, configurations resulting from energy minimization calculations agreed extremely well with the experimentally determined structures. Changes in unit-cell parameters were always smaller than the e.s.d.'s with which they were measured. The same held for the centre of mass translation. Only the overall rotation of molecules in form *B* converged to values slightly different from those of input (max. $\theta_{\text{mol}} = 1.0^\circ$).

Calculated values for the lattice energy of both phases differed considerably, that calculated for phase *A* being 30% lower than that calculated for phase *B* ($E_A = -439$, $E_B = -347$ kJ mol⁻¹). This is in agreement with previous considerations about a better packing for the former.

We gratefully thank Dr E. Castellano, from the Instituto de Física e Química de São Carlos, Brazil, for data collection and Dr A. Nonzioli, from Laboratories Laplex Argentina, for having drawn our attention to the problem.

References

- BONNAUD, B., PROUTIERE, A., VIANI, R., MONNIER, M., BODOT, H. & AYCARD, J. (1987). *Acta Cryst.* **C43**, 1549-1552.
 BOUGÉARD, D. (1984). *Chem. Phys.* **83**, 303-308.
 BURGOS, E. & RIGHINI, R. (1983). *Chem. Phys. Lett.* **96**, 584-590.
 GEISER, U., WANG, H., HAMMOND, E., FIRESTONE, M., BENO, M., CARLSON, K., NUÑEZ, L. & WILLIAMS, J. (1987). *Acta Cryst.* **C43**, 656-659.
 KAWAMOTO, A., TANAKA, J. & TANAKA, M. (1987). *Acta Cryst.* **C43**, 205-207.
 MIRSKAYA, K. V. (1973). *Tetrahedron*, **29**, 679-682.
 Nihon Nohyaku Co. Ltd (1984). *Properties of Non-crystalline Malotilate*. Jpn. Kokai Tokkio Koho JP 59 16,820 [84 16,820].
 SHELDRIK, G. M. (1976). *SHELX76*. Program for crystal structure determination. Univ. of Cambridge, England.
 SHELDRIK, G. M. (1986). *SHELXS86*. Program for crystal structure solution. Univ. of Göttingen, Federal Republic of Germany.
 TAYLOR, R. & KENNARD, O. (1982). *J. Am. Chem. Soc.* **104**, 5063-5070.
 WILLIAMS, D. E. (1967). *J. Chem. Phys.* **47**, 4680-4684.
 WILLIAMS, D. E. (1972). *Acta Cryst.* **A28**, 629-635.
 WILLIAMS, D. E. (1974). *Acta Cryst.* **A30**, 71-77.

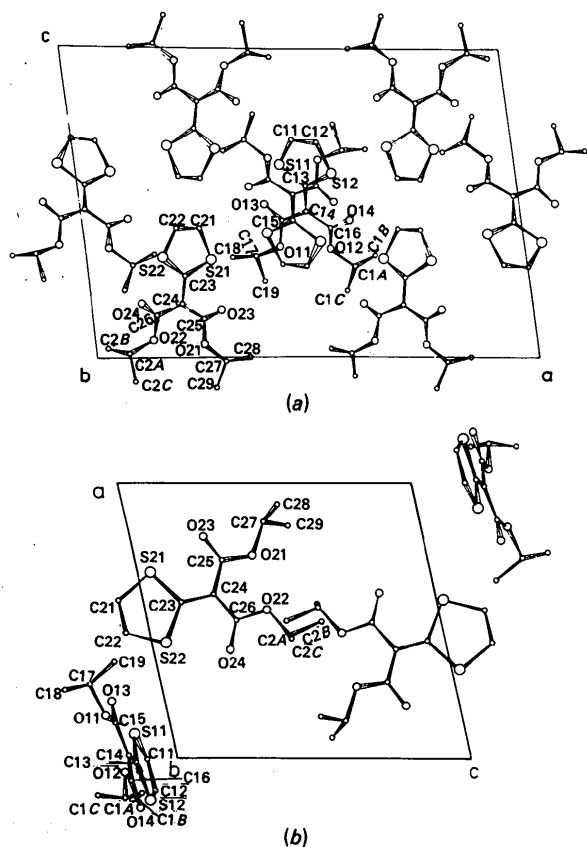


Fig. 1. Projection of the structures along *b*, showing atom numbering as well as differences in packing. (a) Form *A*, monoclinic. (b) Form *B*, triclinic.